Arch. Metall. Mater. **63** (2018), 3, 1235-1242

DOI: 10.24425/123796

H. FUKS*#, S.M. KACZMAREK*, G. LENIEC*, J. MICHALSKI**, ***,
B. KUCHARSKA****, P. WACH**

MAGNETIC PROPERTIES OF STEEL BALL SAMPLES, INVESTIGATED BEFORE AND AFTER NITRIDING

Group of steel balls with different chemical composition, diameters and nitriding treatment parameters were investigated with using magnetic resonance and magnetization methods. Emerging nitrided regions consists of diffusion and surface layer of iron nitrides. The thickness of the individual layers depends on the type of steel and process parameters.

Resonance signal shape and position were successfully described in the ferromagnetic resonance regime expected for dense iron magnetic system. Influence of the sample size, thermal treatment and carbon content on the absorption signal has been analyzed.

Significant magnetic anisotropy has been revealed, as well as non-usual increasing of the magnetization as a function of temperature. It suggests, that overall antiferromagnetic ordering, destroyed by thermal movement, lead to increasing of the ferromagnetic region.

Keywords: EPR-FMR, magnetization, iron, nitriding surface

1. Introduction

The nitriding is a thermo-chemical treatment of the steel, which improves its wear resistance, corrosion resistance and hardness [1-4]. Gas nitriding is a thermo-chemical processing of steel implemented in the temperature range 400-600°C.

At a constant temperature, depending on the value of the nitriding potential, the subsurface iron nitride layer formed may consist of only the γ'-Fe_4N phase or a mixture of phases γ'-Fe_4N and ε-$Fe_{2-3}N$. A diffusion zone is formed under the iron nitride layer, in which nitrogen is dissolved interstitially in a ferritic matrix and carbonitrides of iron and alloying elements occur. The thickness and phase composition of the layers of iron nitrides are decisive on the resistance to corrosion and the abrasive wear of steel after nitriding. The diffusion zone, in the case of alloy steels, increases the fatigue strength of steel [5].

Class description of nitride layers per AMS 2759/10A is [6]:

1.3.1 Class 0

No white layer permitted. (Not recommended for stainless steels.)

1.3.2 Class 1

0.0005 inch (0.013 mm) maximum white layer thickness permitted.

1.3.3 Class 2

0.001 inch (0.025 mm) maximum white layer thickness permitted.

Obtaining these types of layers requires the application of appropriate process parameters, i.e. selecting the appropriate values of the nitriding potential (N_p) for the process temperature set. Mutual relations of the nitriding potential and temperature result from the Lehrer system [7] and for carbon steel and low-alloy steel are as follows:

- Increase of the solution layer α, without nitrides γ' and ε, takes place with nitriding potential $N_p < N_p{}^{\alpha/\gamma'}$ where $N_p{}^{\alpha/\gamma'}$ means the potential corresponding to the boundaries of the phase stability areas α/γ' according to the Lehrer system $T - N_p$.
- Increase of layer γ' takes place when the nitriding potential N_p assumes the values within the phase stability area γ' ($N_p{}^{\alpha/\gamma'} < N_p < N_p{}^{\gamma'/\varepsilon}$), $N_p{}^{\gamma'/\varepsilon}$ means potential corresponding to the boundaries of the phase stability area γ'/ε according to the Lehrer system $T - N_p$.
- Increase of layer ε occurs when the nitriding potential N_p assumes the values within the phase stability area ε ($N_p > N_p{}^{\gamma'/\varepsilon}$) according to the Lehrer system $T - N_p$.

The surface layer (core shell) appearing after nitriding treatment affects the magnetic and electric properties of the steel [2]. In this paper there are presented the results of magnetic and electric studies of steel ball samples underwent nitriding treatment.

The samples, both before and after thermal treatment, were investigated by using EPR and magnetization (SQUID) techniques. The aim of the presented work was to find some general relations between different chemical composition of a steel,

* WEST POMERANIAN UNIVERSITY OF TECHNOLOGY, 17 PIASTÓW AV., 70-310 SZCZECIN, POLAND
** WARSAW UNIVERSITY OF LIFE SCIENCES, 166 NOWOURSYNOWSKA STR., 02-787 WARSZAWA, POLAND
*** INSTITUTE OF PRECISION MECHANICS, 3 DUCHNICKA STR., 01-796 WARSZAWA, POLAND
**** CZESTOCHOWA UNIVERSITY OF TECHNOLOGY, 42-200 CZĘSTOCHOWA, POLAND
# Corresponding author: fux@zut.edu.pl

different diameters of balls, different procedure of a thermal treatment, different depths of core shells formed as an effect of the above process, and magnetic properties concluded from the EPR and SQUID investigations.

2. Experimental

AISI 1010, AISI 1085, AISI 52100 and AISI 420 steels in the form of balls, with chemical composition and diameters as shown in Table 1, were subjected to nitriding processes.

The controlled gas nitriding (CGN) processes were carried out in an Nx609 type industrial soaking furnace with working space dimensions of ϕ 600×900 mm. Test steel samples were nitrided in two-stage processes that differed in temperature, time and nitriding potential in ammonia-dissociated ammonia atmosphere (NH_3/NH_{3zd}). The basic parameters of the nitriding processes are shown in Table 2. Figure 1 shows changes of temperature (Fig. 1a) and nitriding potential N_p (Fig. 1b) as a function of nitriding process time for processes: Nx1021, Nx1025 and Nx1063.

After the nitriding processes, the steel balls were subjected to standard physical metallurgy and XRD examinations. The nitrided layer structural examinations were conducted using a Zeiss Neophot 2 optical microscope on Nital-etched microsections, and included also the thickness measurement of the nitride layers formed in the nitriding process. Phase composition of white layer (nitride layer) and their thickness are shown in Table 3.

Magnetic resonance experiment was performed with using conventional X–band Bruker ELEXSYS E 500 CW–spectrome-

TABLE 1

Chemical composition of steels used in the tests

Grade steel	Sample No	Φ (mm)	Element contents in wt. %						
			C	Mn	Si	P	S	Ni	Cr
AISI 1010	AISI_85	2.00	0.10	0.5	0.1	0.04	0.05	—	—
	AISI_91	2.50							
AISI 1085	AISI_89	2.50	0.85	0.9	0.3	0.04	0.05	—	—
AISI 420-C	AISI_88	2.38	0.47	0.9	1.0	0.04	0.03	0.9	13.5
	AISI_90	1.00							
AISI 52100	AISI_92	1.00	1.0	0.4	0.3	0.02	0.02	—	1.5
	AISI_93	2.50							
	AISI_94	3.00							

TABLE 2

The basic parameters of the nitriding processes

Process No.	Parameters of process Stage I			Parameters of process Stage II			Inlet atmosphere
	T [°C]	t [h]	N_p [atm$^{-0,5}$]	T [°C]	t [h]	N_p [atm$^{-0,5}$]	
Nx1021	580	5	3.20	600	11	0.50	NH_3/NH_{3zd}
Nx1025	490	4	12.5	520	20	0.50	NH_3/NH_{3zd}
Nx1063	540	2	9.0	540	17	1,5	NH_3/NH_{3zd}

TABLE 3

Phase composition of white layer (nitride layer) and their thickness found for processes Nx1021, 1025 and Nx1063

Grade AISI	Sample No.	Φ (mm)	Nx1021		Nx1025		Nx1063	
			g_{mp} (µm)	PC WL	g_{mp} (µm)	PC WL	g_{mp} (µm)	PC WL
AISI 1010	AISI_85	2,0			6,9	Fe_4N-γ'		
AISI 1010	AISI_91	2,5			7,5	Fe_4N-γ'		
AISI 1085	AISI_89	2,5	20.0	Fe_4N-γ'	8,1	Fe_4N-γ'		
AISI 420-C	AISI_88	2,381	8.5-16.5	Fe_4N-γ' $Fe_{2\text{-}3}N$-ε	g_{mp} = 0,0 DL = 0÷70	Fe(N)		
AISI 420-C	AISI_90	1,0	6.5	Fe_4N-γ' $Fe_{2\text{-}3}N$-ε	g_{mp} = 0,0 DL = 0÷30	Fe(N)		
AISI 52100	AISI_92	1,0					17,6	Fe_4N
AISI 52100	AISI_93	2,5					16,2	Fe_4N
AISI 52100	AISI94	3,0					14,7	Fe_4N

g_{mp} – thickness of nitride layer (white layer)
PC WL – phase composition of white layer (nitride layer)
DL – diffusion layer

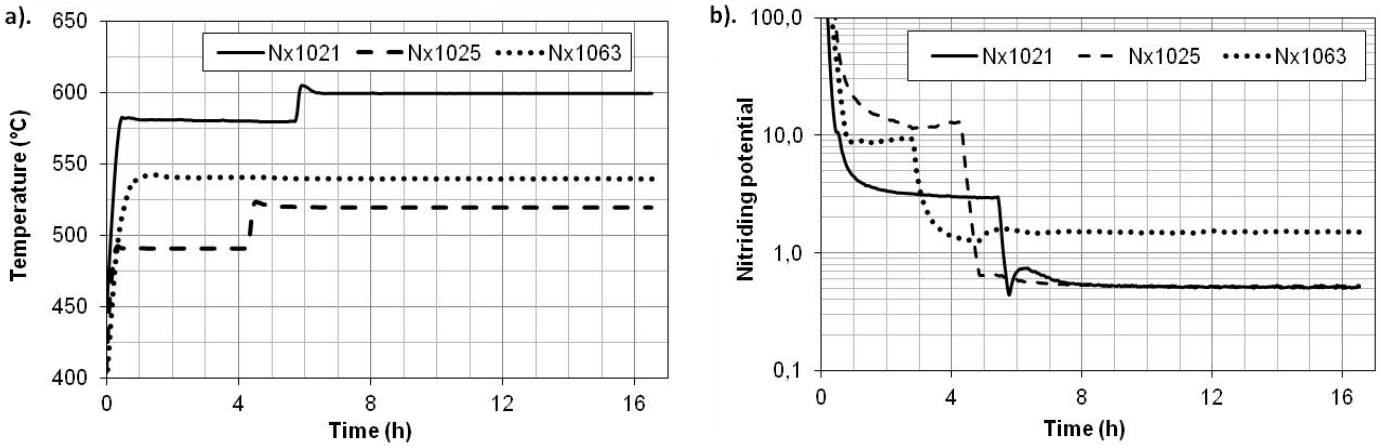

Fig. 1. Changes of temperature T (a) and nitriding potential N_p (b) as a function of nitriding process time for processes: Nx1021, Nx1025 and Nx1063

ter operating at 9.5 GHz with 100 kHz magnetic field modulation. First derivative of the absorption spectra have been recorded as a function of the applied magnetic field within a 0-1.4 T range. Temperature dependences of the spectra were recorded with using Oxford Instrument ESP helium-, nitrogen-flow cryostat in a range of 10-300 K.

The static (dc) magnetic susceptibility measurements were carried out using a Quantum Design MPMS XL–7 with EverCool Magnetic Property Measurement System. The measurements were recorded for temperatures up to 300 K and magnetic fields in a range of 1–500 mT. The dc susceptibilities were measured in the zero-field-cooling (ZFC) and field-cooling (FC) modes.

3. Results

3.1. EPR-FMR resonance results

Magnetic resonance experiment is usually treated in terms of electron paramagnetic resonance (EPR) or ferromagnetic resonance (FMR), depending on a density of responsible magnetic centers. In the case of steel samples the FMR convention is more proper. The FMR spectra (Figs. 2-4) revealed an existence of wide and intense signals observed at a whole accessible temperature range 10-300 K. Fig. 2 presents comparison between spectra of different "non-modified" balls, i.e. samples without nitriding

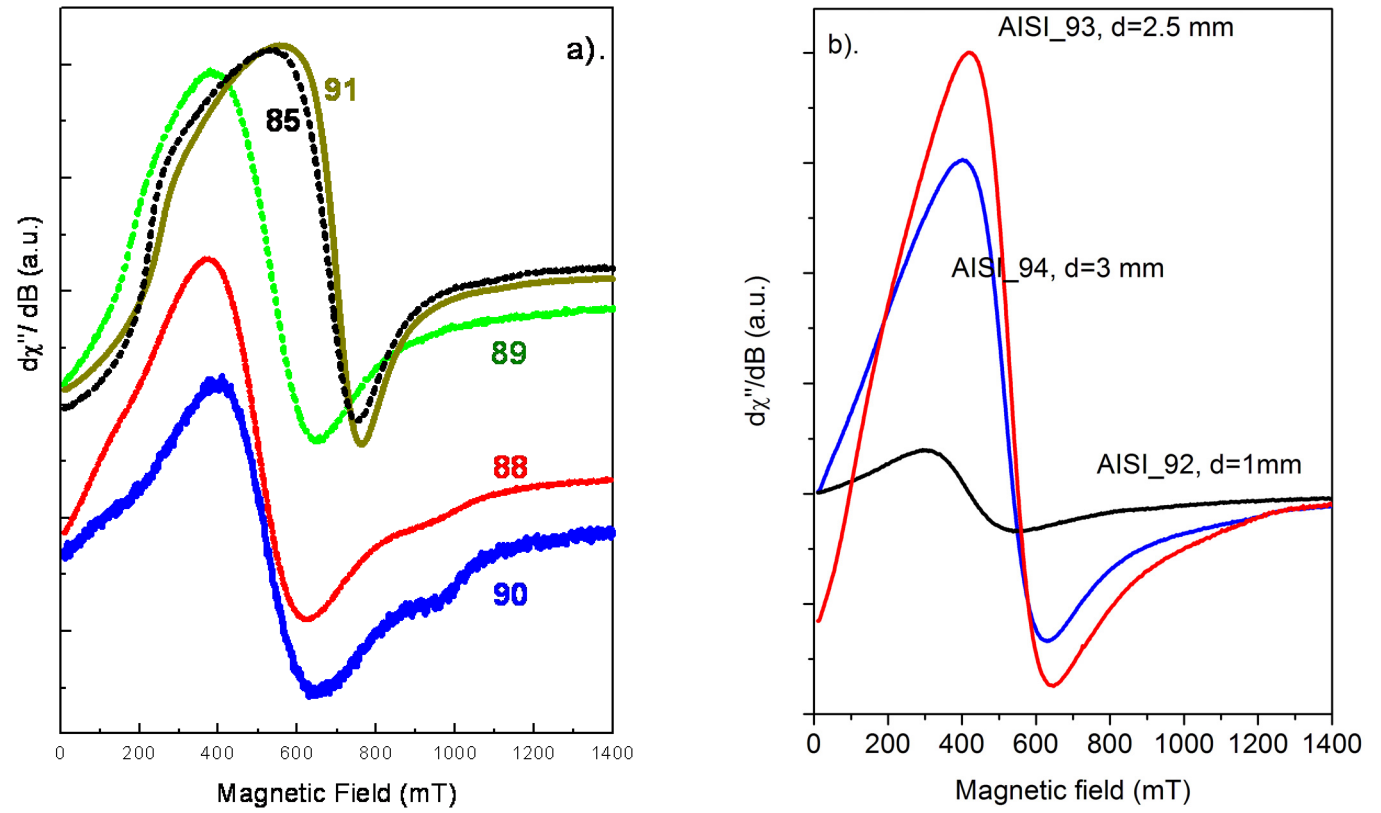

Fig. 2. a). FMR spectra of steel balls AISI_85-91 before nitriding process (non-modified balls) recorded at temperature c.a. 80 K, b). FMR spectra of non-modified balls AISI_92-94 recorded at room temperature

treatment application. According to results presented in Fig. 2a, the resonance signals could be divided into two groups: less symmetric signals located at magnetic field position c.a. 700 mT and more symmetric signals at c.a. 550 mT magnetic fields.

Comparing such FMR results with properties described in Tab. 1 one can conclude, that the main reason of the discrepancy between two groups of spectra may be different carbon content. Indeed, samples: 85 and 91, possessing EPR signals being less symmetric and located at higher magnetic fields, are simultaneously characterized by relatively lower carbon content among presented groups of balls. It indicates, that even insignificant changes of carbon contribution could moderate magnetic properties of such steel enabling to observe it in FMR resonance experiment.

The influence of other magnetic ions as Mn and Cr is also worth of considering, as both ions in FMR experiment are expected to give a resonance signal. But in a case of dense iron system, as we presently mentioned, the influence of additional magnetic ions was rather insignificant due to relatively low intensity and significant widening of the resonance line caused by iron. Some exception could be done for the samples No. 88 and 90, where chromium doping achieves value of c.a. 13.5% (see Tab. 1). Indeed, resonance lines of both samples, presented in Fig. 2a, possess a characteristic disturbance in the form of additional weak signals located near 100 mT and 900 mT magnetic field positions. Such extra weak signals could be ascribed to the randomly distributed chromium ions and, as easy to see, have no influence on the overall iron signal shape. Similar chromium signals we observed earlier in scheelite type phosphates doped by Cr ions [8], where resonance lines near 100 mT and 900 mT we ascribed to the chromium ions located in the interstitial crystallographic position.

Analyzing the overall shape of the resonance lines, one can see, that the "non-modified" ball materials usually possess very complex FMR signal, being far from a standard Lorentzian function. Supposing the model taking into account existence of generally isolated Fe ions, the asymmetry of the resonance signal could be explained by very high conductivity of steel, leading to creation of skin currents under EPR experiment. Such phenomenon was described by Dyson [9] and examined in further EPR experiment [10]. According to the theory, symmetric Lorentzian line is distorted due to non-uniform distribution of

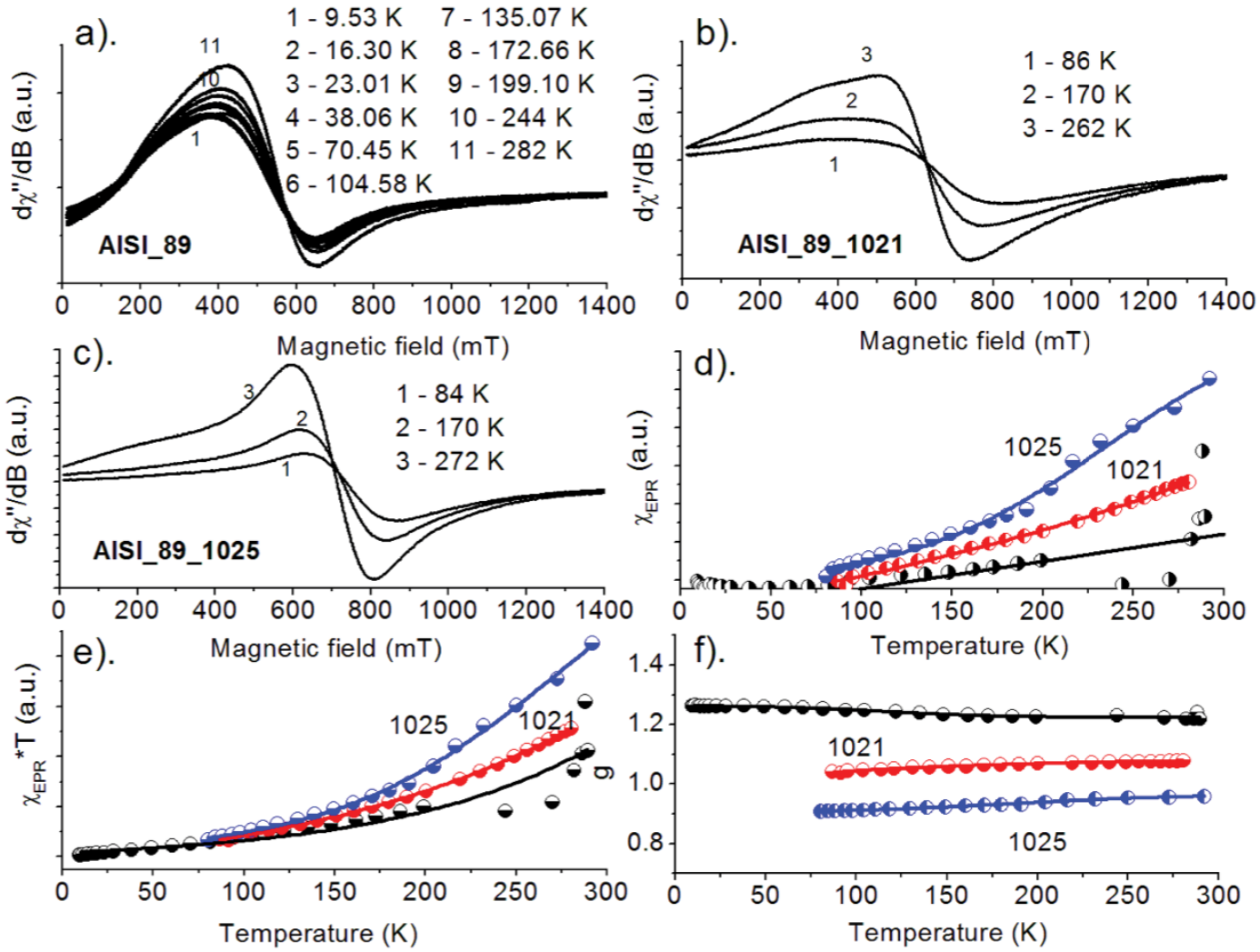

Fig. 3. FMR spectra of sample AISI_89: non-modified (a), after Nx1021 process (b) after Nx1025 process (c). temperature dependence of: integrated intensity (d), product of the integrated intensity with temperature (e), position of resonance lines expressed by effective spectroscopic g-factor (f)

the microwave field in the sample. The level of the asymmetry, among many factors, depends on the relation between size of a sample and skin depth. Contribution of asymmetric Dyson-like (Dysonian) function to overall EPR line is expected to be weaker for smaller samples. Indeed, among the spectra presented in Fig. 2 the spectra of samples: AISI_90 and 92 have relatively most symmetric resonance signal. These balls possess significantly lowest size: 1 mm in diameter, comparing to 2-3 mm for the other samples (Tab. 1).

The EPR signal of isolated Fe magnetic ions could be located at c.a. 340 mT, which corresponds to spectroscopic factor value of $g_{eff} \approx 2$ [11,12]. From the other hands, if EPR resonance signal originates from iron complexes, the observed EPR signals are shifted towards lower magnetic fields, with $g_{eff} > 4$ [11,12]. It is completely inconsistent with our case, even if Dysonian component is taken into account.

As it was mentioned earlier, the investigated steel balls should be treated in terms of dense Fe magnetic system. In the case, experimental spectra should be described as a result of FMR absorption experiment. As can be seen (Fig. 2), resonance positions of the FMR lines are strongly shifted, probably due to the presence of internal magnetic fields, including dipolar and demagnetization components. The asymmetry of the absorption signals, observed near lower magnetic fields (Fig. 2) could be a result of high sensitivity of the samples to the initial sample magnetization. Similar shapes of the resonance signals and their explanation were reported for example in [13] and [14], where Fe_3C magnetic agglomerates were analyzed in terms of FMR regime.

The resonance signals of all investigated samples were characterized as functions of processing temperature and nitriding process. Good example of such investigations is a set of pictures shown in Fig. 3 describing temperature dependences of representative sample AISI_89. As could be seen, FMR signal increases as a function of temperature (Figs 3a-d), which is completely inconsistent with Curie-Weiss relation expected for simple paramagnetic species. Similar increase of $\chi(T)$ relation was reported in [13] and explained by forming of ferromagnetic agglomerates. In our case an increasing of $\chi(T)$ could be explained by similar mechanism. As the AISI steel materials are expected to possess a long-range antiferromagnetic (AFM) interaction between magnetic species [15], an increase in temperature causes destroying of overall AFM order and ferromagnetic (FM) imperfection of the structure appears. Additional discussion of this question will be presented later in the present paper, after its supplementation with SQUID measurement results.

Another conclusion emerging from Fig. 3a-c is increasing the symmetry of overall FMR signal after nitriding process, where level of the symmetry is higher if thermal treatment was undergone at lower temperature and longer time (process Nx1025). Simultaneously, nitriding processes lead to moving the FMR signal towards higher magnetic field (lower g value, see Fig. 3f). It clearly suggests that both factors: temperature and time of exposition in nitriding atmosphere have influence on magnetic properties of the investigated steel materials. The process Nx1025, characterized by relatively longer time of heating under lower temperature, leads to higher level of homogeneity of responsible magnetic centers and thus FMR signal is more symmetric.

The observed enhancement of the resonance lineshape symmetry caused by nitriding treatment is characteristic for all considered ball samples and all three nitriding processes.

The parameters of resonance signal, presented in Fig. 3d-f, were estimated through the integration of absorption line and calculation of the resonance position. Detailed analysis, including all components of the overall signal, is difficult in this case. FMR signal shape is inconsistent with simple magnetic model represented by Lorentzian function. As was mentioned earlier, the FMR resonance line could be disturbed by some factors, like initial magnetization or high conductivity of a sample. In the latter case, modified Lorentzian equation represented by Dysonian function could be adequate, but other attempts to resolve a dense iron magnetic system are sometimes testified, for example, Landau-Lifshitz function [16].

Fig. 4 presents results of simulation of the FMR resonance signals with using two Dysonian lines for the following samples: AISI_89 (1021), AISI_89 (1025) and AISI_93 (1063). As could be seen the result of simulation is rather satisfying. Low lying component is strongly distorted, whereas second one, centered at higher magnetic field, is close to the Lorentzian shape.

So, approximation the FMR resonance signal with using a composition of two components is simplest way to solve the problem, sometimes successfully, as it was done, for example, in [14]. But we should keep in mind, that iron samples consists of many magnetically non-equivalent magnetic centers, so overall FMR signal may be a superposition of more than two components.

3.2. Magnetization results

The results obtained from a magnetization experiment (SQUID) revealed increase of the magnetic susceptibility, M, as a function of temperature. Such behavior, shared to all samples, is presented in Figs 5 and 6 for samples AISI_88 and AISI_92-94. The observed increase of the magnetization with increasing temperature is consistent with previously observed temperature behavior of the FMR signal intensity (see Fig. 3d), but the SQUID experiment provided us some additional information.

Magnetization was measured at two modes of cooling: ZFC and FC under relatively weak magnetic field $H = 10$ mT. As could be seen, $M(T)$ relation reveals significant bifurcation between FC and ZFC modes, extended with cooling of the sample (Fig. 5a). Bifurcation tends to disappear at temperatures close to 300 K. The discrepancy between FC and ZFC modes indicates on significant magnetic anisotropy, being higher at lower temperatures, which is destroyed at higher temperatures.

The increase of magnetic susceptibility as a function of temperature could be explained by appearing of AFM structure in the investigated samples. According to earlier reports concerning similar kind of steel [15], such materials possess specific magnetic composition. In these materials minority of FM components

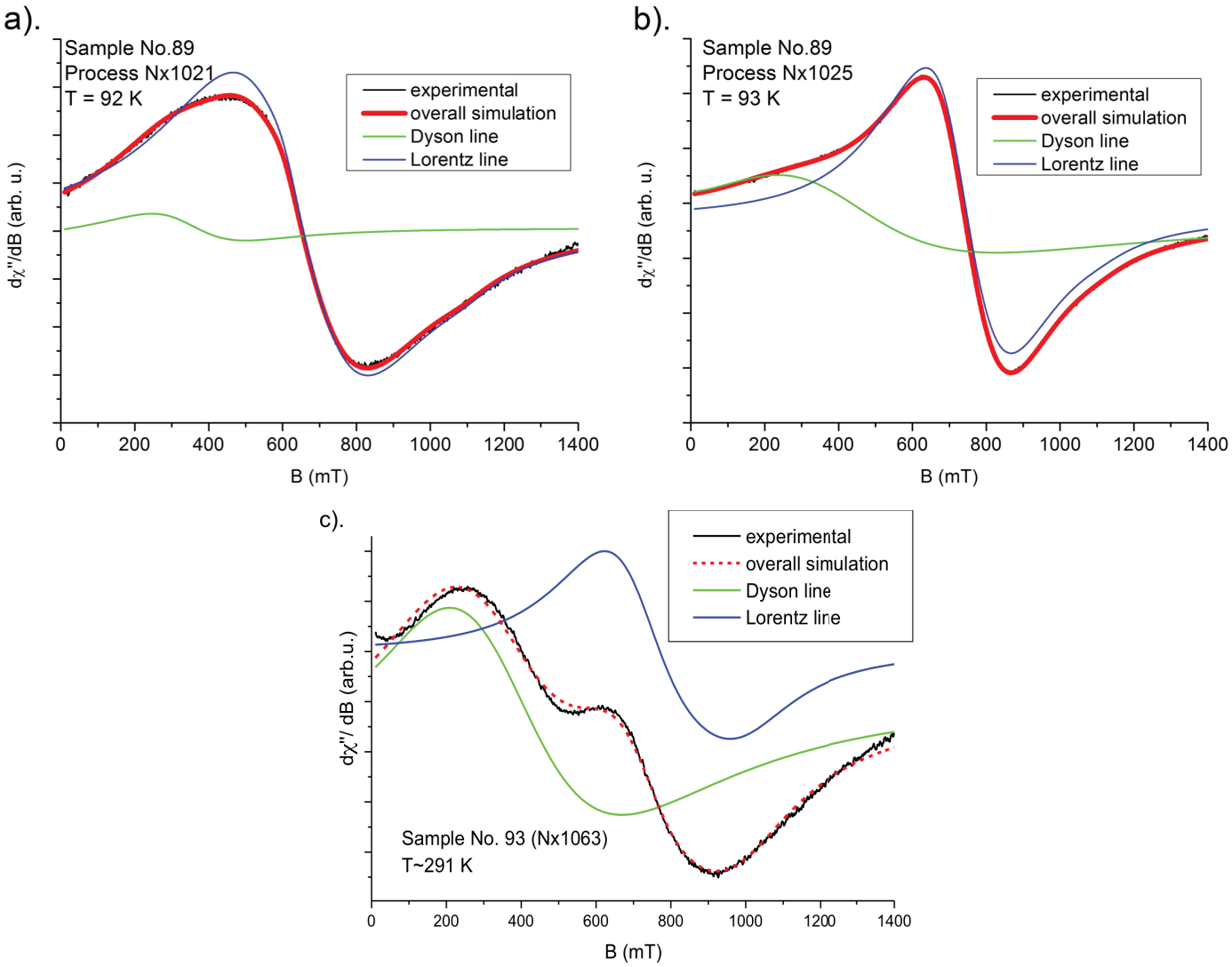

Fig. 4. Simulation of the FMR signal as a superposition of two components: asymmetric Dysonian function and symmetric Lorentzian function for the samples: a). AISI_89 (1021), b). AISI_89 (1025), c). AISI_93 (1063). Two former FMR spectra were recorded at about 90 K, whereas the latter at room temperature

occur as an imperfection in overall AFM structure. Thus, AFM ordering is destroyed with increasing temperature and overall magnetization is enhanced. Similar behavior of $M(T)$ relation was observed in other Fe containing materials [17], where increase the $M(T)$ was explained by creation of Fe^{2+} ions in the structure built of Fe^{3+}.

The above explanation, supposing that AFM structure is destroyed by FM imperfection seems to be confirmed if one compare Fig. 4a and 4b. Indeed, plot representing $M(T)$ relation, registered under circumstances of not so strong operating magnetic fields (10 mT, Fig. 5a) is completely different if experiment is performed under 500 mT (Fig. 5b). In this latter case the $M(T)$ increases with increasing temperature at the beginning and at temperatures above 50 K the tendency is suddenly broken and $M(T)$ decreases. It is consistent with the mechanism, in which the initial AFM ordering is easy destroyed by strong external magnetic field. FM ordering between magnetic species is embedded and sample behaves as typical ferromagnet. The results shown in Fig. 5a,b are similar as presented in [18], where magnetic properties of γ-Fe_2O_3 nanocomposites were examined and explained by coupling between nanoparticles leading to building of large magnetic aggregates.

Influence of a sample diameter on the $M(T)$ plot is shown in Fig. 6a. As could be seen, the bifurcation observed at lower temperatures is relatively higher for lower ball diameter. Sample AISI_92, characterized by lowest diameter, simultaneously possess highest nitriding layer size (see Tab. 3). It means, that the ratio between overall diameter and width of nitriding layer may be a critical factor for this phenomenon, where magnetic anisotropy is enhanced thanks to increasing contribution of surface nitrogen.

In Fig. 6b we presented the dependence of $M(T)$ on different values of magnetic field from 10 to 200 mT for AISI_92 sample with lowest diameter. Magnetic fields lower than 200 mT do not change the increasing character of magnetization, but $M(T)$ plot tends to reverse itself to known shape, observed in Fig. 5b. It confirms the destroying role of strong magnetic field on overall AFM ordering in presented steel materials.

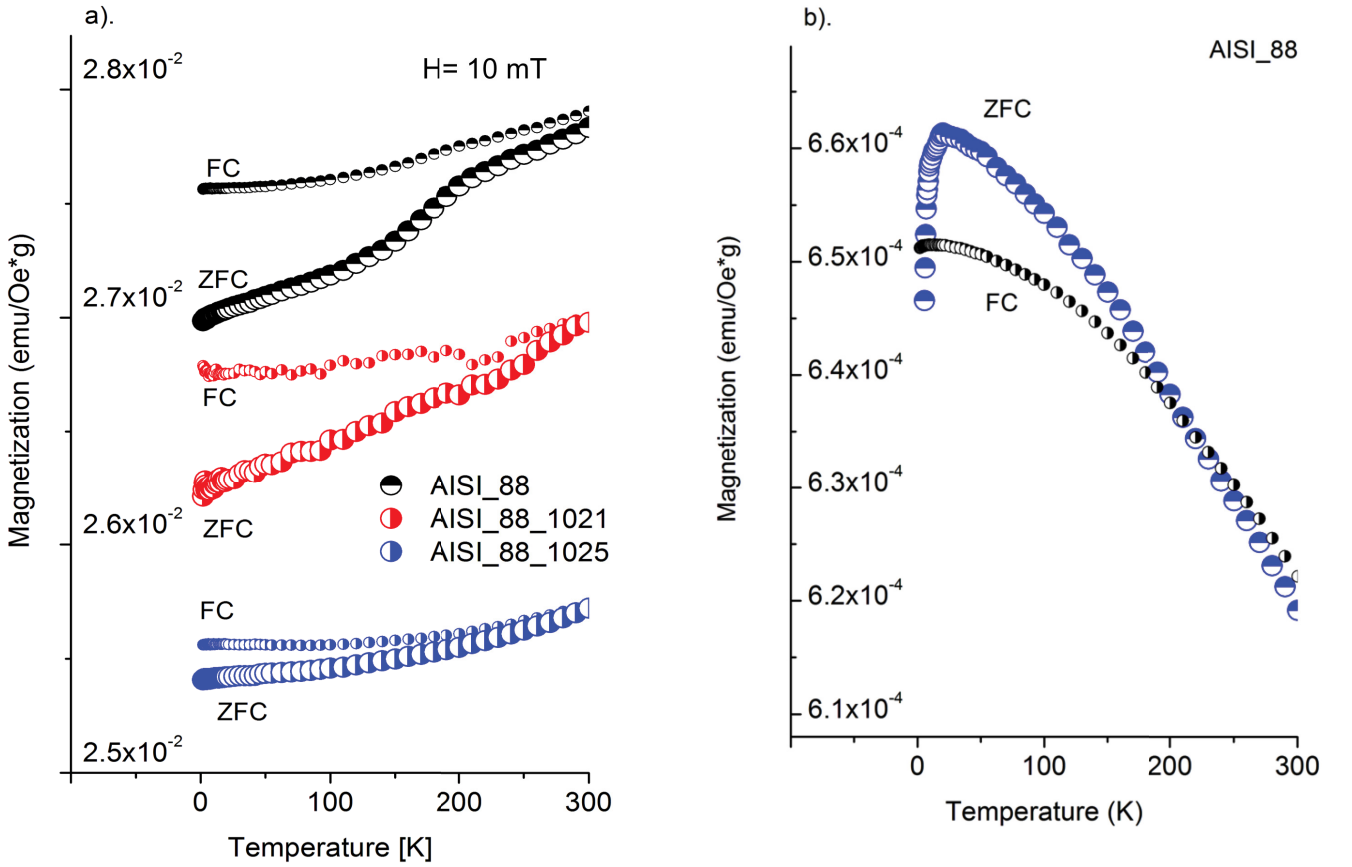

Fig. 5. The $M(T)$ dependence registered for the samples: a). AISI_88, AISI_88_Nx1021 and AISI_88_Nx1025 for H =10 mT, b). AISI_88 sample for H = 500 mT

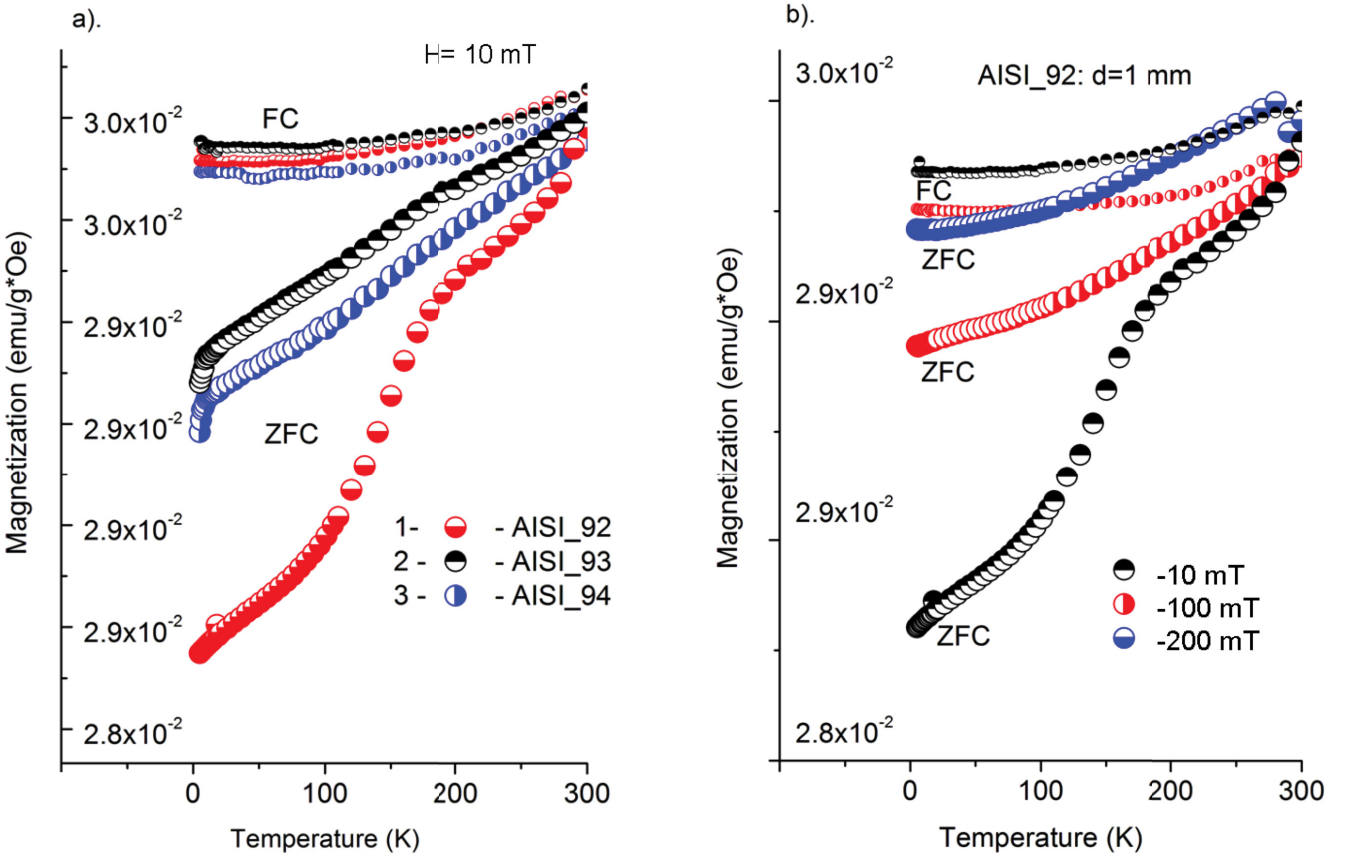

Fig. 6. Magnetization: a) AISI samples possessing a different size for H = 10 mT, b). AISI_92 for H = 10, 100 and 200 mT

4. Conclusions

Concentration of carbon in investigated steel materials has an influence on their magnetic properties. Lower C content leads to less symmetric FMR signals, located at higher magnetic fields, whereas higher C content gives opposite results. Asymmetry of the resonance signal observed in samples possessing lower carbon content is connected with higher conduction of steel and increasing role of circular current in FMR experiment. Resonance condition, modified in steel materials by contribution of internal (demagnetization and dipolar) magnetic fields, is sensitive to the C content too. Thus, position of overall resonance signal is lower or higher, depending on higher or lower carbon concentration, respectively.

Materials with similar C content gives more symmetric resonance signal if possess lower size. It could be explained by lower circular current effect for small samples.

Thermal treatment (nitriding) leads to increasing the homogeneity of magnetic objects, which results from increasing symmetry of the observed FMR signal comparing to the signal of non-modified samples. Among three kinds of thermal treatments the process Nx1025 gives relatively more symmetric FMR signals comparing to two other processes. It indicates that longer time of treatment with moderate temperature leads to the ordering among magnetic species.

FMR signal, even for most symmetric cases, was simulated with using at least two Lorentzian components, modified to the form of Dysonian function. Complexity of the overall FMR signal means, that homogeneity of existing magnetic species is far from perfection. Existence of Dysonian components indicates on significant contribution of circular current to the FMR signal. One can remember, that applying the Dysonian functions to FMR signal approximation is not satisfying for samples with low carbon content. In this case more sophisticated model should be proposed.

FMR signal intensity, similarly as magnetization value, increases with increasing testing temperature. It is completely inconsistent with Curie-Weiss behavior predicted for paramagnetic sites. Increasing of the signal is explained as a process of destroying of overall AFM ordering among iron magnetic species. As temperature increases building of the region with FM ordering takes place. Such mechanism, where FM region appears as a perturbation of the AFM structure seems to be confirmed by completely different behavior of $M(T)$ relation if experiment is performed under strong magnetic field. In the condition of strong external field, AFM ordering is destroyed very fast and sample behaves as a typical ferromagnet.

Significant bifurcation between FC and AFC modes in $M(T)$ experiment indicates on large magnetic anisotropy of responsible magnetic species at low temperatures. It suggests, that AFM ordering is a combination of short and long distance interactions between iron magnetic species. Low scale magnetic particles couple each other, to form large aggregates within metallic grains.

According to presented results, EPR-FMR is enough sensitive technique to register differences in physical properties of steel samples underwent nitriding with different process parameters. Other factors like: chemical composition, sample diameter, nitriding layer size, also have an influence onto registered magnetic properties, thus presented magnetic methods seems to be useful testing tools of this type of steel materials. It is worth of noting, that spherical shape of the investigated samples was not obligatory. Next step of our study includes other shapes of steel samples.

REFERENCES

[1] E.J. Mittemeijer, J.T. Slycke, Surface Engineering **12** (2), 152-162 (1996).

[2] M. Betiuk, J. Tacikowski, Inżynieria powierzchni **17** (3), 39-45 (2012).

[3] J. Senatorski, J. Tacikowski, E. Kasprzycka, B. Bogdański, Inżynieria Powierzchni **18** (2), 63-66 (2013).

[4] J. Michalski, K. Burdyński, P. Wach, Z. Łataś, Archives of Metallurgy and Materiale **60** (2), 747-754 (2015).

[5] G. Mońka, J. Tacikowski, J. Michalski, Inżynieria Powierzchni **1**, 7-13 (2014).

[6] Norm AMS 2759/10A, Automated Gaseous Nitriding Controlled by Nitriding Potential, Issued: May 1999, Revised: June 2006.

[7] B. Langenhan, H.J. Spies, Einfluss der Nitrierbedingungen auf Morphologie und Struktur von Verbindungsschichten auf Vergütungsstählen, HTM **7**, 337-343 (1992).

[8] S. M. Kaczmarek, G. Leniec, H. Fuks, T. Skibiński, A. Pelczarska, P. Godlewska, J. Hanuza, I. Szczygieł, World Journal of Applied Physics **2** (1), 7-18 (2017).

[9] F.J. Dyson, Phys. Rev. **98** (2), 349-359 (1955).

[10] G. Feher, A.F. Kip, Phys. Rev. **98** (2), 337-351 (1955).

[11] R.S. Muralidhara, C.R. Kesavulu, J.I. Rao, R.V. Anavekar, R.P.S. Chakradhar, Journal of Physics and Chemistry in Solids **71**, 1651-1655 (2010).

[12] E. Bletsa, M. Solakidou, M. Louloudi, Y. Deligiannakis, Chem. Phys. Letters **649**, 48-52 (2016).

[13] N. Guskos, J. Typek, M. Maryniak, U. Narkiewicz, W. Arabczyk, I. Kucharewicz, J. Phys: Conf. Series **10**, 151-154 (2005).

[14] U. Narkiewicz, N. Guskos, W. Arabczyk, J. Typek, T. Bodziony, W. Konicki, G. Gąsiorek, I. Kucharewicz, E.A. Anagnostakis, Carbon **42**, 11127-1132 (2004).

[15] J. Crangle, A. Fogarty, M.J. Taylor, J. Magn. and Magn. Mater. **111**, 255-259 (1992).

[16] N. Guskos, J. Typek, G. Zolnierkiewicz, K. Wardal, A. Guskos, P. Berczynski, D. Petridis, Materials Science-Poland **31** (4), 587-594 (2013).

[17] Z. Jian, N.P. Kumar, M. Zhong, H. Yemin, P.V. Reddy, J. Supercond. Nov. Magn. **28**, 2627-2635 (2015).

[18] N. Guskos, V. Likodimos, S. Glenis, M. Maryniak, M. Baran, R. Szymczak, Z. Rosłaniec, M. Kwiatkowska, D. Petridis, J. Nanosci. and Nanotechnol. **8**, 2127-2134 (2008).